Commun Transp Res

Research Article

Investigating the car-following behavior of electric vehicles with one-pedal driving

Tianle Zhu, Handong Yao✉, Wenjie Zhao, Qianwen Li

Cite this article: Zhu T L, Yao H, Zhao W J, et al. *Commun Transp Res* 2026, **6**(2): 9640030. https://doi.org/10.26599/COMMTR.2026.9640030

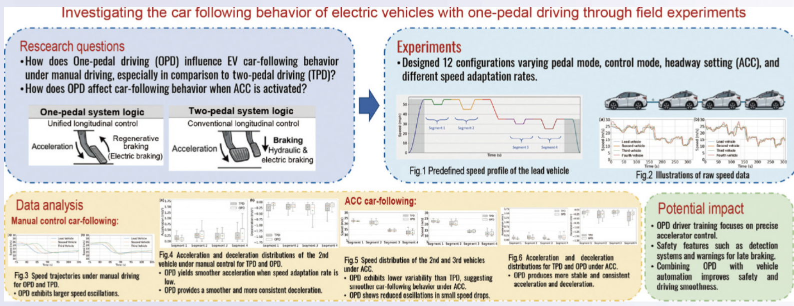

ABSTRACT: With the rapid growth of the electric vehicle (EV) market, one-pedal driving (OPD) has become a widely adopted feature in modern EVs. This study addresses two key questions of OPD: (1) Its influence on EV car-following behavior and (2) its interaction with adaptive cruise control (ACC). To explore these questions, field experiments were conducted to empirically compare one-pedal and two-pedal driving (TPD) under both manual control and ACC settings. Statistical and comparative analyses reveal significant behavioral differences across control settings. Under manual control, OPD produces more pronounced speed oscillations and sharper decelerations with quicker responses, primarily because acceleration and braking are managed solely through the accelerator pedal. Drivers, especially those less experienced, struggle with fine speed modulation, resulting in greater variability. These findings highlight the need to account for driver familiarity and heterogeneity when modeling OPD behavior. Under ACC, OPD yields narrower distributions of speed, acceleration, and spacing, indicating smoother and more conservative control, while both modes exhibit similar response delays. This suggests that integrating OPD with ACC can attenuate disturbance propagation and enhance platoon stability. The findings contribute to a deeper understanding of the influence of OPD on car-following behavior and provide practical insights for developing and tuning ACC systems that effectively leverage regenerative braking to improve traffic flow efficiency and system stability.

KEYWORDS: regenerative braking; adaptive cruise control (ACC); manual control; pedal driving; car-following

1 Introduction

Growing public awareness of environmental sustainability and the urgent need for energy savings have significantly accelerated the adoption of electric vehicles (EVs) worldwide. Reflecting this trend, the share of EVs in global automobile sales surged from merely 4% in 2020 to an impressive 18% in 2023, marking a rapid and sustained growth in the transition toward cleaner transportation solutions (Wang and Witlox, 2025). This rising public interest is reinforced by growing concern over climate change, with many countries planning to ban the sale of combustion engine vehicles (Li et al., 2024; Ruan and Lv, 2022). A key technological feature of EVs is regenerative braking systems (RBSs). Unlike traditional friction braking with brake pedals, RBS allows EVs to recover kinetic energy during deceleration and convert it into electrical energy for storage. This improves energy efficiency and extends the driving range, which is especially valuable in urban settings where the speed is low and frequent braking is common (Hamada and Orhan, 2022).

Building upon RBS, one-pedal driving (OPD) has emerged as an advanced and energy-efficient control strategy increasingly adopted in EVs (e.g., Tesla, Ford Mustang Mach-E, and Kia Niro). In this mode, the accelerator pedal alone is used for both acceleration and deceleration, allowing drivers to manage speed and braking without engaging the brake pedal under non-emergency conditions. According to Wang et al. (2015), OPD demonstrated significant energy savings of up to 22% in urban environments and 13% on rural roads, compared to RBS used in two-pedal driving (TPD), where the accelerator controls acceleration, and the brake pedal manages deceleration. These gains are primarily attributed to improved driving dynamics and more consistent kinetic energy recovery, especially in stop-and-go driving scenarios. Beyond its energy savings, OPD can also enhance driving safety in typical urban driving environments. According to Ma et al. (2025), simulations demonstrated that OPD yielded a lower collision rate under mild deceleration scenarios on urban roads compared to TPD.

Despite these advantages, Ma et al. (2025) highlighted several limitations of OPD in emergency scenarios where abrupt deceleration is needed. Specifically, when the lead vehicle's

College of Engineering, University of Georgia, Athens GA 30602, USA.

✉ Corresponding author. E-mail: Handong.Yao@uga.edu

Received: December 3, 2025; Revised: March 17, 2026; Accepted: May 20, 2026

Nomenclature

EV	Electric vehicle
RBS	Regenerative braking systems
OPD	One-pedal driving
TPD	Two-pedal driving
ACC	Adaptive cruise control
DTW	Dynamic time warping

deceleration exceeded 0.5 or 0.75 g, or when the lead vehicle switched from mild to sudden braking, the collision rate in OPD was significantly higher than that in TPD. This elevated risk is primarily attributed to delayed braking behavior: Drivers in OPD tend to rely excessively on regenerative braking and typically do not press the brake pedal until the time-to-collision drops to a small, nearly constant threshold. Such system-induced delayed brake activation reduces the reaction time for applying sufficient braking force, thereby increasing the likelihood of rear-end collisions in emergency scenarios.

Understanding the car-following behavior of EVs with OPD is essential for evaluating their impact on collision risk, traffic flow stability, and energy consumption in transportation systems (Brackstone and McDonald, 1999; Treiber et al., 2000). Car-following behavior can be characterized by several key factors, such as speed, spacing, and reaction time (Brackstone and McDonald, 1999; Fayolle et al., 2022; Orosz et al., 2010). These factors influence how speed perturbations propagate through a traffic flow, potentially triggering stop-and-go waves and reducing the overall roadway capacity (Li, 2022). Accurately capturing these factors is fundamental for developing and calibrating car-following models, which in turn enable realistic simulations and inform the design of safer, more efficient transportation systems (Gunter et al., 2020a). Moreover, extracting implicit human behaviors from sequence data can further enhance this modeling fidelity. For instance, recent research has demonstrated this by using language models to learn driver routing patterns (Liu et al., 2023).

Most existing studies on OPD have focused on single-vehicle dynamics. While a few prior studies have shown that EVs exhibit distinct car-following behavior, such as faster acceleration response and earlier deceleration initiation, compared to internal combustion engine (ICE) vehicles (Li et al., 2019), little to no research has examined the car-following behavior of EVs with OPD. This gap raises a research question: How does OPD influence EV car-following behavior, especially in comparison to TPD?

Another key feature that can influence car-following behavior is adaptive cruise control (ACC) (Gunter et al., 2020b; Rajamani, 2006). By automating longitudinal control—maintaining a desired time gap or distance from the preceding vehicle and adjusting speed through throttle and braking interventions—ACC produces more consistent spacing and speed-adjustment patterns compared to manual control. This uniformity helps reduce speed fluctuations and enhances the stability of traffic flow. Recent field experiments have highlighted the distinct car-following behavior of EVs with ACC. For example, Lapardhaja et al. (2023) demonstrated that EVs with ACC can sustain shorter and more stable headways even under traffic oscillations, enabled by a rapid motor torque response and regenerative braking. Researchers have modeled such behavior using microscopic models such as the intelligent driver model (IDM) (Treiber et al., 2000) and the optimal velocity relative velocity (OVRV) model (Gunter et al., 2020b; Milanés and Shladover, 2014). Zare et al. (2023) calibrated both models using field data from EVs with ACC and found that the simple and linear OVRV model better captured EV car-following behavior with ACC. While ACC controls both throttle and braking to enhance longitudinal vehicle behavior, OPD introduces a distinct control paradigm by relying solely on the accelerator pedal for both acceleration and deceleration. This fundamental difference in control strategy may lead to unique interactions when OPD is used in conjunction with ACC, potentially affecting car-following behavior. This raises an important additional question: How does OPD influence the car-following behavior of EVs with ACC?

As summarized in Table 1, prior research has examined EV dynamics, ACC performance, or OPD energy efficiency individually; however, no existing studies have simultaneously investigated how OPD affects EV car-following behavior or explicitly addressed these two research questions. To address this gap, this study conducted platoon experiments involving three following EVs equipped with both OPD and ACC. Field data were collected under both manual control and ACC conditions to enable a comprehensive comparison of car-following behavior between OPD and TPD modes. We first employed dynamic time

Table 1 Expanded overview of related studies and their focus areas

Ref.	Focus area			
	EV	ACC	OPD	Car-following
Wang and Witlox (2025)	✓	—	—	—
Hamada and Orhan (2022)	✓	—	—	—
Wang et al. (2015)	✓	—	✓	—
Ma et al. (2025)	✓	—	✓	—
Li et al. (2019)	✓	—	—	✓
Orosz et al. (2010)	—	—	—	✓
Fayolle et al. (2022)	—	—	—	✓
Li (2022)	—	—	—	✓
Gunter et al. (2020a)	—	✓	—	✓
Gunter et al. (2020b)	✓	✓	—	✓
Lapardhaja et al. (2023)	✓	✓	—	✓
Zare et al. (2023)	✓	✓	—	✓
Treiber et al. (2000)	—	✓	—	✓
Rajamani (2006)	—	✓	—	✓
This study	✓	✓	✓	✓

warping (DTW) to examine the consistency of trajectory data across Experiments and then applied a nonparametric Mann–Whitney U test to verify whether significant differences in car-following behavior existed between OPD and TPD under both manual control and ACC settings. Further empirical analyses of speed evolution, acceleration/deceleration patterns, and spacing revealed that, under manual control, OPD induces greater variability and stronger deceleration. Under ACC, OPD tends to produce smoother but more conservative following behavior. These findings can improve the modeling and simulation of EV car-following behavior with OPD, supporting the design and tuning of ACC systems tailored to OPD-equipped vehicles and enhancing the performance of emerging transportation systems.

In summary, this study makes the following key contributions:

• This study collected the first set of platoon trajectory data for EVs operating in both OPD and TPD under both manual control and ACC settings. The full dataset is publicly available at https://github.com/UGA-MOBILITY-LAB/ev-car-following-opd.

• To the best of our knowledge, this is the first study to investigate OPD in EV car-following behavior.

2 Data collection

Since no existing datasets are available to address the above two research questions, this study conducted platoon experiments specifically designed to capture EV car-following behavior under both OPD and TPD across manual control and ACC settings, following similar settings (Chon Kan-Munoz et al., 2021). The tests took place on a straight, low-traffic segment of Georgia State Route 72 near the University of Georgia (Fig. 1) selected for its flat terrain, clear lane markings, and minimal external disturbances. All data were collected during off-peak hours to reduce the influence of surrounding traffic. This choice of studied corridor was intended to isolate the fundamental car-following dynamics and control characteristics inherent to OPD compared to TPD, which provides a clean baseline for leader–follower interactions before examining more complex urban traffic scenarios.

The experiments involved a fleet consisting of one ICE vehicle and three EVs (Fig. 2). The lead vehicle was a 2021 Lexus UX 200 equipped with ACC. The following EVs included a 2024 Ford Mustang Mach-E and two 2023 Kia Niro EVs, all equipped with both OPD and ACC. This configuration allowed us to test OPD and TPD under both manual control and ACC settings. During the experiments, each vehicle's trajectory data were collected using a RaceBox global positioning system (GPS) device with a 10 Hz sampling rate. The GPS installation setup is shown in Fig. 2. In practice, a positional accuracy of approximately 10 cm at a 10 Hz sampling rate corresponds to a velocity noise level of approximately 0.1–0.3 m/s. Therefore, the influence of velocity measurement errors is considered negligible in this study. To ensure consistency, all GPS devices were mounted in the same position across vehicles. The vehicle order within the platoon remained unchanged throughout all experimental runs. To maintain a consistent baseline and minimize the impact of varying familiarity levels, we recruited three participants through a random selection process on a university campus. All participants were current students with an average age of 24. These drivers were highly proficient in TPD, with their licensed driving experience ranging from 4 to 6 years. Critically, all participating drivers had prior experience with EV driving but were novices to OPD without prior experience before the experiment. The limited sample size and the homogeneous driver group may constrain the generalizability of the findings. Future experiments will include a larger and more diverse participant pool, incorporating drivers with varying levels of OPD familiarity and experience, to better capture individual adaptation patterns.

To compare OPD and TPD, the platoon experiments were divided into two trials. In the first trial, all following EVs operated in OPD and were tested under both ACC and manual control settings. To account for the impact of traffic oscillations, each test was further divided into two scenarios: One featuring a high-speed adaptation rate and the other featuring a low-speed adaptation rate. In the second trial, the EVs operated in TPD, with all other experimental conditions held constant. For tests with ACC activated, two headway settings—the shortest and longest available—were evaluated. A detailed summary of all experimental configurations is provided in Table 2.

During the experiments, the lead vehicle consistently operated with cruise control and was adjusted manually following a predefined speed profile. Fig. 3 illustrates the predefined speed profile. Each test began with the lead vehicle accelerating from rest (0 mph) to 55 mph to establish free-flow conditions. It then varied its speed between 50–55 mph (Segment 1 in Fig. 3) and 45–55 mph (Segment 2 in Fig. 3). This was followed by a transitional deceleration phase from 35 to 55 mph to simulate a shift to lower-

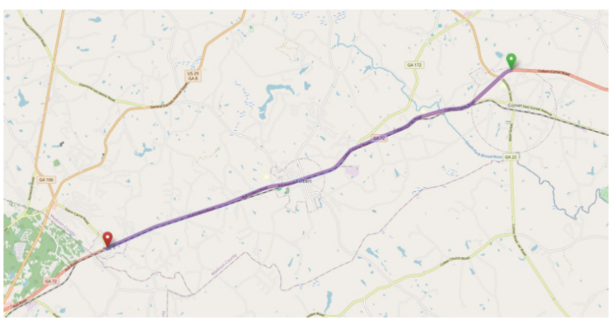

Fig. 1 Experimental road segment on GA-72 (source: OpenStreetMap).

Fig. 2 Two images on the right show the following EVs, while the left image shows the windshield-mounted RaceBox GPS unit.

Table 2 Summary of the experimental design. The study included 12 experiments covering all combinations of pedal mode (OPD vs. TPD), control mode (ACC vs. manual), headway setting (longest vs. shortest for ACC, N/A for manual), and speed adaptation rate (low, e.g., $0.5\ m/s^2$ vs. high, e.g., $1.5\ m/s^2$)

Experiment number	Pedal mode	Control mode	Headway setting	Speed adaptation rate
1	OPD	ACC	Longest	Low
2	OPD	ACC	Longest	High
3	TPD	ACC	Longest	Low
4	TPD	ACC	Longest	High
5	OPD	ACC	Shortest	Low
6	OPD	ACC	Shortest	High
7	TPD	ACC	Shortest	Low
8	TPD	ACC	Shortest	High
9	OPD	Manual	—	Low
10	OPD	Manual	—	High
11	TPD	Manual	—	Low
12	TPD	Manual	—	High

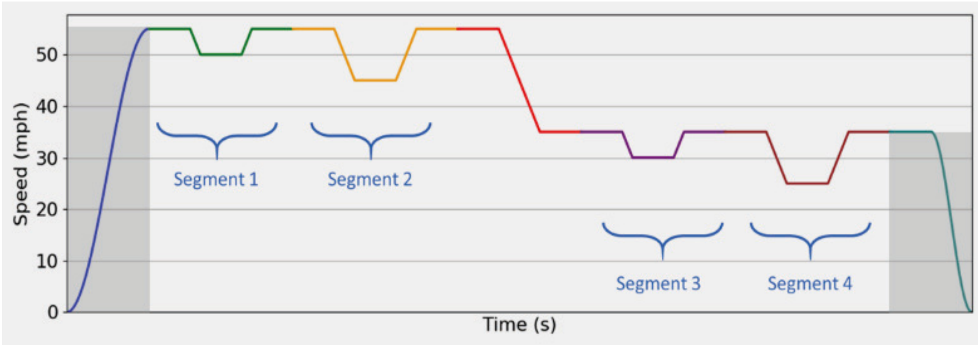

Fig. 3 Predefined speed profile of the lead vehicle.

speed conditions. After reestablishing free-flow conditions, the lead vehicle adjusted its speed between 30–35 mph (Segment 3 in Fig. 3) and 25–35 mph (Segment 4 in Fig. 3). Finally, it decelerated from 35 mph to a complete stop.

Fig. 4 presents two examples of the raw speed data with OPD and TPD. The lead vehicle follows the predefined speed profile, and the speed disturbance patterns of the following EVs align well with the expected car-following patterns.

3 Data consistency and reliability analysis

3.1 Data consistency on the lead vehicle

To ensure that the paired experiments were comparable, DTW was applied to analyze the lead-vehicle speed profiles. DTW is a distance-based time-series analysis method that measures the similarity between two temporal sequences by allowing nonlinear alignments along the time axis. This method has been widely adopted in vehicle trajectory analysis for investigating driver behavior heterogeneity and temporal alignment between leader–follower pairs (Taylor et al., 2015). Unlike traditional point-to-point comparisons, such as Euclidean distance or correlation, DTW compensates for minor time shifts and duration differences, providing a robust measure of trajectory similarity. Formally, given two speed sequences $Q = (q_1, q_2, \ldots, q_i)$ and $C = (c_1, c_2, \ldots, c_j)$, DTW seeks an optimal warping path d, that minimizes the total alignment cost:

$$\mathrm{DTW}\,(Q, C) = \min \sqrt{\sum_{i,j} d(q_i, c_j)^2} \tag{1}$$

where $d(q_i, c_j)$ is the distance of the element of the warping path.

In this study, the lead vehicle was asked to follow the same predefined speed profile in each paired experiment (e.g., 1–3, 2–4). Therefore, data consistency is verified by measuring the normalized DTW distance between the lead vehicle trajectories in a paired experiment. The DTW distance was normalized by the total sequence length because each paired experiment had slightly different durations, and normalization ensured that the results represented the average temporal deviation rather than being biased by sequence length. The resulting normalized DTW distance reflects the average discrepancy in speed patterns, with smaller values indicating higher trajectory consistency.

To verify the consistency of the experimental conditions, compare the DTW distance between the lead vehicles of the two experiments with the DTW distance between the lead and following vehicles within the same experimental pair. According to the car-following model proposed by Newell (2002), a following vehicle reproduces the trajectory of the lead vehicle in space, offset by a constant time and distance. Under the Newell model, the speed profiles of the leader and the follower are mathematically identical in shape, with the lead–follower DTW distance representing the inherent spatial-temporal shift. Consequently, if the DTW distance between the lead vehicles from two different experiments is smaller than the lead–follower DTW distance within a single experiment, it demonstrates that the variations between experimental trials are even lower than the displacement defined by the car-following logic. This relates directly to the DTW results: The deterministic and consistent nature of the Newell model provides a rigorous benchmark for trajectory similarity, confirming that lead vehicle behavior is highly consistent and that the experimental conditions are comparable across different sessions.

Table 3 presents the normalized DTW distances between lead vehicles across experiment pairs and the minimum normalized DTW distances between the lead and second vehicles within each experiment. Since each experiment contains two lead–follower pairs, only the minimum value is selected. Across both ACC and manual control conditions, the lead–lead distances are consistently smaller than the corresponding lead–follower values, indicating that the lead vehicles' trajectories under OPD and TPD are highly consistent. Since the lead and second vehicles typically exhibit similar driving patterns, this confirms that cross-experimental differences in lead vehicle behavior are minor and can be regarded as a stable baseline for subsequent analyses.

3.2 Data reliability of following vehicles

Before conducting the systematic analysis, it is essential to verify

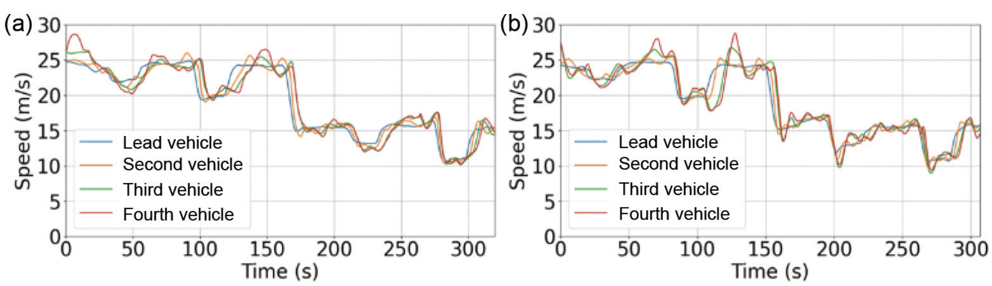

Fig. 4 Illustrations of raw speed data for different pedal modes in manual control: (a) TPD and (b) OPD.

Table 3 Normalized DTW distances between lead vehicles across experimental pairs and the minimum normalized DTW distances between lead and second vehicles within each experiment. Lower lead–lead distances relative to lead–follower values indicate consistent lead vehicle behavior across OPD and TPD conditions

Exp A	Exp B	A description	B description	Lead–lead	Lead–follower
1	3	OPD-ACC	TPD-ACC	0.112	0.176
2	4	OPD-ACC	TPD-ACC	0.038	0.179
5	7	OPD-ACC	TPD-ACC	0.084	0.222
6	8	OPD-ACC	TPD-ACC	0.087	0.199
9	11	OPD-manual	TPD-manual	0.096	0.325
10	12	OPD-manual	TPD-manual	0.192	0.212

the reliability of the collected data. In this section, we present the experiments that exhibited potential offsets or incorrect setup configurations.

Fig. 5e illustrates the spacing distribution between the following vehicles in experiment 5. Notably, the third and fourth vehicles display markedly different distributions, despite being of the same brand and model operating under ACC control. Such discrepancies are unlikely to arise under identical control modes and headway settings. This observation suggests that the third vehicle may have inadvertently remained in the longest headway setting or that a GPS offset occurred during data collection. Consequently, experiment 5 was excluded from the analysis, and its paired experiment (experiment 7) was also omitted due to the loss of the pairing relationship.

Figs. 5k and 5l present the distribution of spacing between the following vehicles in experiments 11 and 12 under manual control. The distributions of the fourth vehicle are too close to zero, with minimum values of 1.12 and 0.31 m, which may have been caused by a GPS offset. In this case, data from the fourth vehicle were excluded from the subsequent analysis under manual driving conditions.

4 Car-following behavior analysis

4.1 Statistical analysis for OPD and TPD

To examine the influence of control modes on EV car-following behavior, this study analyze their significant differences. Since DTW is primarily suited for assessing equivalence in trajectory patterns rather than conducting statistical inference, a formal hypothesis testing framework was adopted. Furthermore, the Kolmogorov–Smirnov (KS) test ($p < 0.05$) indicated that the collected data violated the normality assumption required for a parametric t-test. Thus, a nonparametric alternative, the Mann–Whitney U test, was employed.

The Mann–Whitney U test (also known as the Wilcoxon rank-sum test) assesses whether two independent samples originate from the same population without assuming normality. This method is particularly appropriate for behavioral and trajectory datasets that often exhibit skewness or non-Gaussian characteristics, offering a robust and interpretable measure of group-level differences between OPD and TPD.

The analysis focused on four key car-following factors, which collectively capture the core dimensions of efficiency, safety, passenger comfort, and traffic flow stability.

1) Speed, where temporal speed profiles were analyzed to assess the speed oscillation under each pedal mode, serving as a key indicator of efficiency.

2) Acceleration, where instantaneous acceleration profiles were examined to capture driver adaptation to control smoothness, which is a primary determinant of passenger comfort and efficiency.

3) Deceleration, where braking responses were examined to capture driver adaptation to regenerative braking, which is related to safety and passenger comfort.

4) Spacing, where the distance between the lead vehicle and the following vehicle was quantified to measure spacing stability and responsiveness, acting as the primary physical buffer for collision risk and the most important determinants of string stability.

4.1.1 Statistical differences in car-following behavior under manual control

Table 4 presents the *p* values of the Mann-Whitney U test for each indicator under manual control. Speed exhibited moderate sensitivity, showing statistically significant differences in most cases but fewer than the other indicators. The exception was the third vehicle in experiment pairs 10–12, likely because the lead vehicle operated under a high-speed adaptation rate in both tests. Consequently, the following vehicle adopted a more conservative control strategy, resulting in similar speed profiles across pedal modes.

Acceleration and deceleration both showed notable differences between OPD and TPD in experiment pairs 9–11, particularly for the second vehicle, which is most directly influenced by the lead vehicle. In contrast, no significant difference in acceleration was observed in experiment pairs 10–12, possibly due to the smoother lead-vehicle behavior under a higher speed adaptation rate.

Among all indicators, spacing demonstrated the highest sensitivity, exhibiting statistically significant differences across nearly all segments and vehicles. This is probably because speed- and acceleration-based indicators are derived from position data and are therefore more affected by measurement and differentiation noise. Beyond these technical factors, spacing serves as a cumulative state variable that integrates relative speed differences over time. In manual control, even slight inconsistencies in how drivers modulate the single pedal compared to the traditional two-pedal system accumulate into more significant and observable variations in spacing than in instantaneous speed or acceleration.

4.1.2 Statistical differences in car-following behavior under ACC

Table 5 presents the *p* values of the Mann-Whitney U test for each indicator under ACC. Speed exhibited significant differences primarily in Experiments pair 1–3, while in other pair, significance was observed mainly for the fourth vehicle. The high-speed adaptation rate settings in Experiment pair 2–4 and 6–8 result in similar speed profiles.

Acceleration only displayed clear differences across all vehicles in experiment pairs 6-8. This is probably because the longer headway setting in experiments 1-4 reduces driver responsiveness to fluctuations ahead, resulting in similar acceleration profiles.

Deceleration results indicated significant differences for all vehicles except in experiment pairs 1–3, where the absence of significance may be attributed to the long headway and low-speed adaptation settings, which mitigated braking variability between pedal modes.

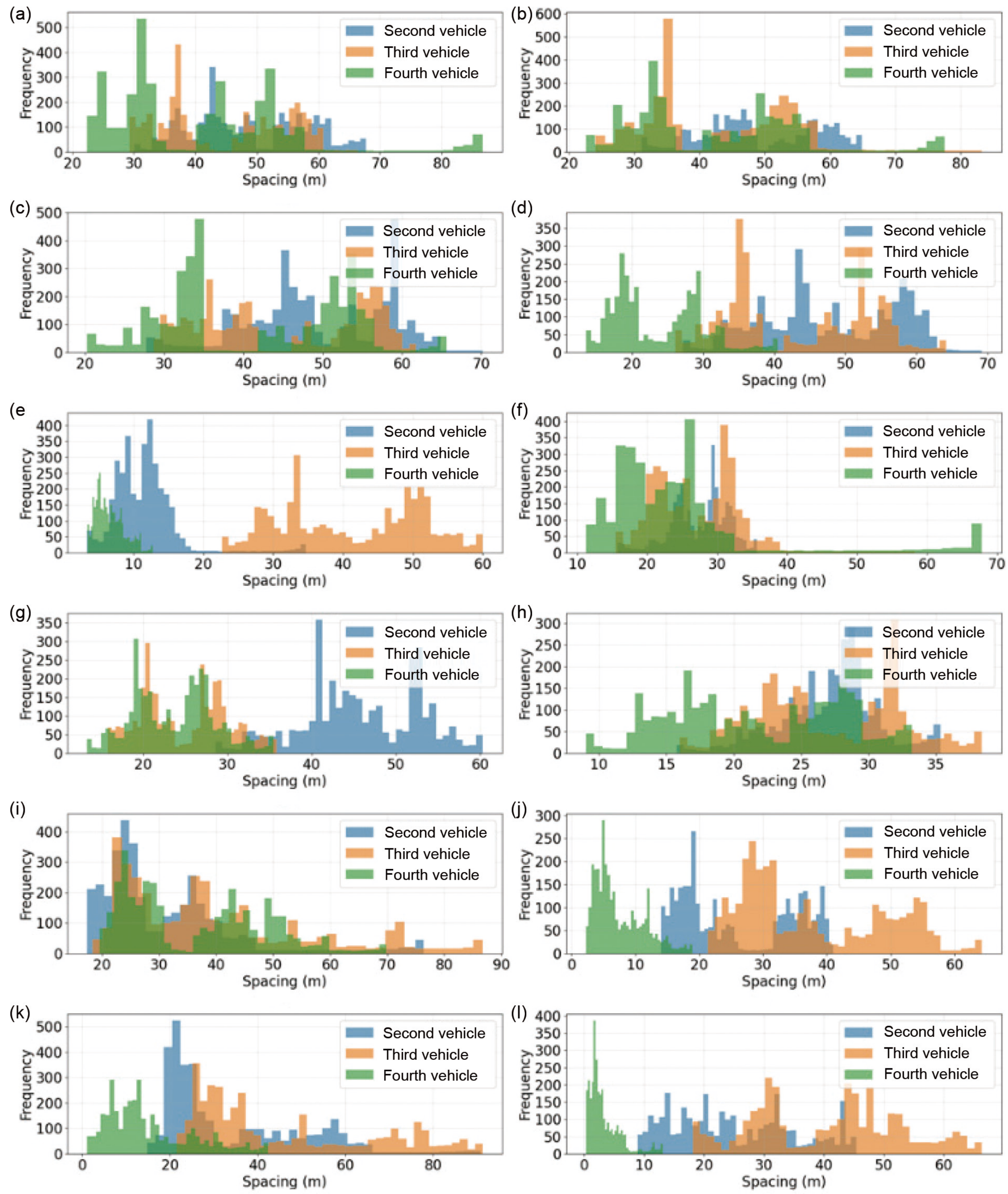

Fig. 5 Spacing distribution of vehicles across Experiments 1–12.

Table 4 Mann–Whitney U test p values under manual control for different Experiment pair

Experiment pair	Indicator	p value	
		Second vehicle	Third vehicle
9 vs. 11	Speed	0.001	0.032
	Acceleration	< 0.001	0.291
	Deceleration	< 0.001	< 0.001
	Spacing	0.019	< 0.001
10 vs. 12	Speed	0.026	0.553
	Acceleration	0.572	0.691
	Deceleration	0.356	< 0.001
	Spacing	< 0.001	< 0.001

Table 5 p values of the Mann–Whitney U tests for each car-following indicator under ACC control. Lower p values indicate stronger differences between OPD and TPD modes

Experiment pair	Indicator	p value		
		Second vehicle	Third vehicle	Fourth vehicle
1 vs. 3	Speed	< 0.001	< 0.001	0.0326
	Acceleration	0.163	0.085	0.009
	Deceleration	0.366	0.870	< 0.001
	Spacing	< 0.001	0.041	< 0.001
2 vs. 4	Speed	0.760	0.420	0.059
	Acceleration	0.445	0.037	0.306
	Deceleration	0.001	0.328	< 0.001
	Spacing	< 0.001	0.003	< 0.001
6 vs. 8	Speed	0.117	0.452	0.007
	Acceleration	0.013	< 0.001	< 0.001
	Deceleration	0.008	< 0.001	< 0.001
	Spacing	< 0.001	0.562	< 0.001

Finally, spacing remained the most sensitive indicator, showing statistically significant differences across most vehicles and experiment pair. This highlights spacing as a robust measure of car-following behavioral differences under different control modes.

In summary, the Mann–Whitney U test results under ACC control indicate that spacing exhibits the most consistent and significant differences across experiments. This is primarily because while the ACC algorithm strictly regulates instantaneous speed and acceleration to follow a target profile, spacing acts as a cumulative indicator that integrates relative speed differences over time. In contrast, acceleration and deceleration show condition-dependent variations influenced by headway and speed adaptation, and speed differences are primarily significant in experiment pairs 1–3, reflecting oscillatory effects in specific vehicles.

Table 6 summarizes the average effect sizes (r) of the Mann-Whitney U tests for all car-following indicators under both ACC and manual control conditions. Overall, spacing exhibits the highest and most variable effect sizes across experiments, particularly in pair 2 vs. 4 ($r = 0.284$) and 10 vs. 12 ($r = 0.103$), indicating that it is the most sensitive indicator to control-mode differences. Acceleration and deceleration show moderate effects in several experiment pairs, with the largest values observed in 6 vs. 8 and 10 vs. 12, suggesting more pronounced behavioral deviations during dynamic speed adjustments. Speed differences, however, remain consistently small ($r < 0.05$) across all conditions, implying that both OPD and TPD maintain similar longitudinal velocity profiles under ACC. This pattern is more obvious under manual control than under ACC, suggesting that while further analysis and modeling for manual control may place greater emphasis on spacing, models under ACC should consider all factors.

4.2 Comparative analysis of OPD and TPD

Following the statistical analysis, a comparative analysis was conducted to further understand the detailed differences in car-following behavior with different pedal and control modes.

4.2.1 Manual control car-following

We first examined the car-following behavior under manual control with OPD and TPD. Figs. 6a and 6b depict an example where the lead vehicle decelerates from 50 to 55 mph at a high-speed adaptation rate setting (e.g., fast deceleration). Under OPD, RBS is activated immediately upon release of the accelerator, prompting the following vehicle to decelerate with minimal reaction delay. In contrast, TPD responses involve a more noticeable lag due to the driver's need to switch from throttle to brake. Figs. 6c and 6d plot the speed trajectories with both high-speed and low-speed segments. Interestingly, drivers using OPD tend to exhibit more pronounced speed oscillations, especially in high-speed segments. This is likely because OPD requires drivers to control both acceleration and deceleration using only the accelerator pedal, which is more sensitive and harder to control speed precisely than a two-pedal system. Moreover, many drivers are in a short-term adaptation phase to OPD, further contributing to the variability. This suggests that the observed oscillations may be a combination of the intrinsic sensitivity of single-pedal control and driver short-term adaptation effect to OPD. Notably, even in low-speed segments, OPD still results in larger speed oscillations compared to TPD. These behavioral patterns are important to consider when understanding EV car-following behavior, as the growing adoption of EVs introduces many drivers who are inexperienced with OPD. Understanding their adaptation process provides valuable insights into how EVs affect transportation systems.

As expected, speed oscillations amplify downstream from the second to the third vehicle, reflecting the typical propagation of disturbances in a platoon. However, the difference between OPD and TPD is not obvious. To better understand the influence of pedal modes, this study then investigate other factors.

Table 6 Average effect sizes (r) of the Mann-Whitney U tests for each car-following indicator under both ACC and manual control conditions. Higher r values indicate stronger behavioral differences between OPD and TPD modes

Indicator	1 vs. 3	2 vs. 4	6 vs. 8	9 vs. 11	10 vs. 12
Speed	0.038	0.013	0.021	0.032	0.018
Acceleration	0.031	0.023	0.060	0.044	0.049
Deceleration	0.021	0.047	0.081	0.081	0.096
Spacing	0.062	0.284	0.044	0.086	0.103

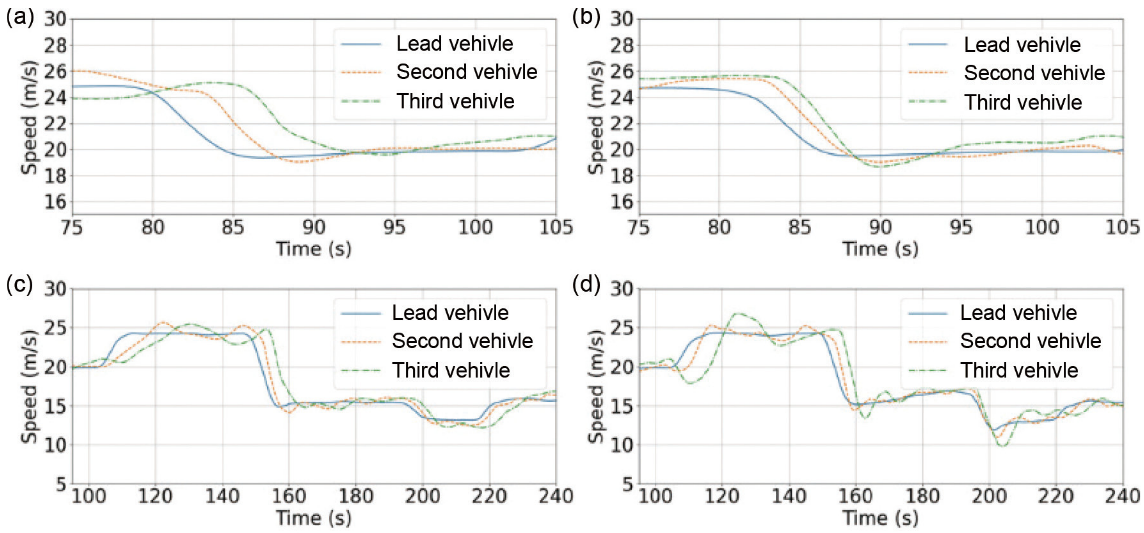

Fig. 6 Speed trajectories under different pedal modes with manual control: the deceleration from 50 to 55 mph (Segment 1) for (a) TPD and (b) OPD in manual control; the high-speed and low-speed profiles for (c) TPD and (d) OPD in manual control.

Table 7 quantify the speed oscillation patterns observed earlier. In both OPD and TPD modes, the third vehicle consistently shows larger speed standard deviations than the second vehicle, indicating the amplification of disturbances as they propagate downstream in the platoon. Comparing the two pedal modes, the differences are not consistent across segments. In Segment 1, OPD shows a much smaller speed variability than TPD, suggesting that the immediate regenerative braking response can reduce the reaction delay under relatively stable conditions. However, in the more dynamic segments (Segments 2–4), the differences between OPD and TPD become less clear, with both modes showing comparable levels of speed variability. Overall, these results suggest that while OPD may help stabilize small speed adjustments, its higher sensitivity and drivers' adaptation process can also contribute to noticeable speed oscillations.

Fig. 7 illustrates the acceleration and deceleration distribution of all vehicles. In Figs. 7a and 7c, the acceleration distributions from the second to the third vehicle are shown. In the high-speed profiles (Segments 1 and 2), the acceleration patterns do not exhibit a consistent trend. However, in the low-speed profiles (Segments 3 and 4), all vehicles show a wider acceleration range under OPD compared to TPD, indicating larger acceleration fluctuations. In low-speed conditions, vehicle speed varies more frequently, making it more difficult for drivers to maintain stable regenerative braking since both stopping and starting are controlled solely by the accelerator pedal. In contrast, under TPD mode, switching from the accelerator to the brake pedal provides a short buffer period, resulting in smoother acceleration behavior.

Table 7 Speed standard deviation of EVs in OPD and TPD modes during manual driving

Segment	Mode	Second vehicle	Third vehicle
Segment 1	OPD	0.405	1.029
Segment 1	TPD	1.484	1.792
Segment 2	OPD	1.755	2.176
Segment 2	TPD	1.535	1.756
Segment 3	OPD	1.041	1.587
Segment 3	TPD	0.886	1.235
Segment 4	OPD	1.551	1.769
Segment 4	TPD	1.860	2.187

Figs. 7b and 7d show the deceleration distributions for the same vehicles. In the high-speed profiles (Segments 1 and 2), the second vehicle exhibits a wider deceleration range, while the third vehicles do not show the same pattern. This difference may be attributed to the vehicle models—the second vehicle being a Ford Mustang Mach-E, whereas the third are Kia Niro EVs—or to variations in individual driving behavior. In the low-speed profiles (Segments 3 and 4), the differences become more pronounced. In Segment 3, where the lead vehicle's speed decreases from 30 to 35 mph, all vehicles under TPD mode display more stable deceleration, likely for the same reason discussed earlier for acceleration in low-speed conditions. However, in Segment 4, the opposite trend appears: Vehicles under OPD mode are more stable. This may indicate that under larger deceleration demands, the regenerative braking of OPD provides a smoother and more consistent deceleration response. Overall, these results suggest that OPD introduces greater variability in longitudinal control at low speeds but offers smoother responses under stronger deceleration. However, due to the small sample size and differences in driver experience with OPD, these findings should be interpreted cautiously. With more practice, drivers may develop better pedal control, reducing this variability. Future studies with more participants and consistent driver training are needed to validate these observations.

Fig. 8 presents the spacing distributions of the second and third vehicles across four segments under TPD and OPD. Several key patterns emerge. First, under TPD, spacing oscillations are more evident in the high-speed segments (segments 1 and 2), while spacing remains relatively stable in the low-speed segments (segments 3 and 4). In contrast, OPD shows noticeable spacing variability even in the low-speed segments, likely due to the increased intrinsic difficulty of precise speed control using only the accelerator pedal and the transitional lack of familiarity among the study's drivers. This variability suggests that OPD may impose higher cognitive and control demands on drivers, resulting in higher potential risks. Spacing oscillations tend to amplify from the second to the third vehicle, reflecting typical disturbance propagation in a platoon. For the second vehicle, both TPD and OPD exhibit similar spacing trends across all segments, although OPD introduces slightly less variability. The third vehicle under OPD shows relatively consistent spacing oscillations across segments, while TPD displays greater fluctuation in high-speed

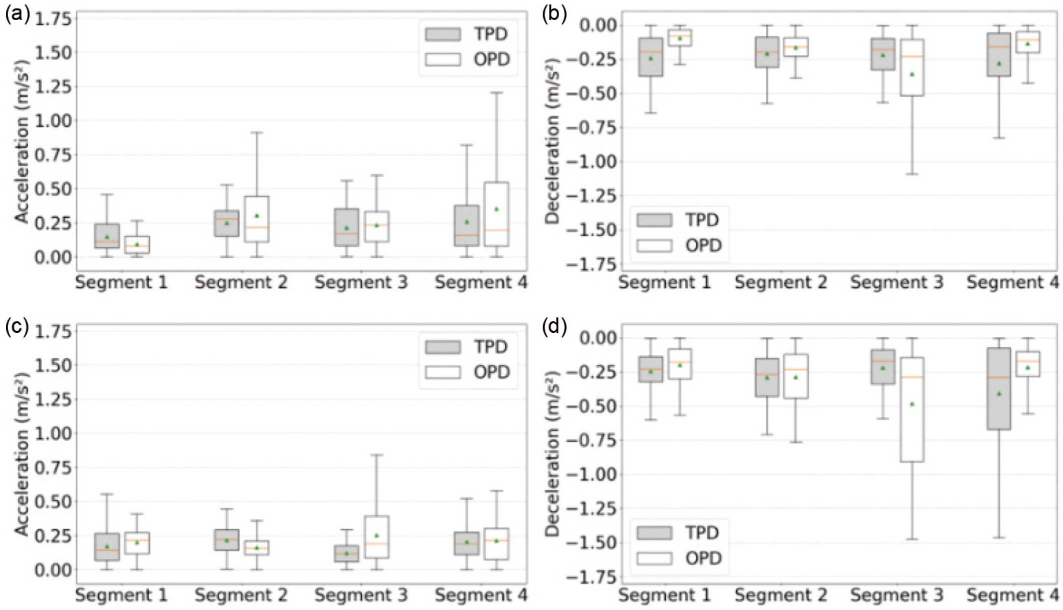

Fig. 7 Acceleration and deceleration distributions for TPD and OPD under manual control. Subplots (a) and (c) illustrate acceleration for the second and third vehicles, respectively, while subplots (b) and (d) depict the corresponding deceleration distributions for the same vehicles.

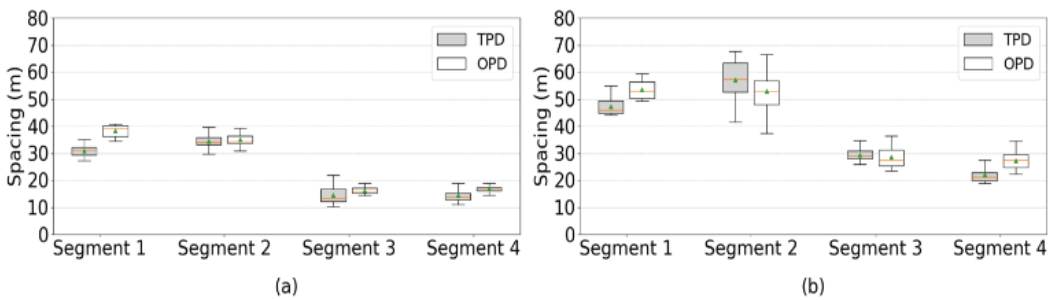

Fig. 8 Spacing distributions for TPD and OPD in manual control: (a) the second and (b) third vehicles.

conditions. The lack of a clear and consistent trend under OPD may be attributed to driver heterogeneity in experience, comfort, and response strategies. Collecting more manual control data may help reveal more generalizable spacing patterns.

4.2.2 ACC car-following

Next, examined the detailed differences between OPD and TPD in ACC. Figs. 9a and 9b illustrate speed trajectories under the longest spacing settings. Overall, the delay across vehicles is minimal in both pedal modes. This is expected, as ACC automates longitudinal control and minimizes driver input, thereby masking some of the behavioral variability observed under manual control.

Figs. 9c–9e illustrate the speed distributions of the second, third, and fourth vehicles under TPD and OPD across four Segments. Overall, OPD exhibits lower variability than TPD, suggesting smoother car-following behavior under ACC. In segments involving smaller speed drops—such as segment 1 (from 50 to 55 mph) and segment 3 (from 30 to 35 mph)—OPD shows reduced oscillations compared to TPD. In contrast, in segments with larger speed drops—segment 2 (from 45 to 55 mph) and segment 4 (from 25 to 35 mph)—both OPD and TPD take longer to respond to greater disturbance, resulting in similar increased variability. These observations suggest that the regenerative braking response and tighter feedback control in OPD-equipped vehicles enable smoother adjustments to moderate speed oscillations.

Table 8 further quantifies the speed variability under ACC for OPD and TPD modes. Consistent with the distribution patterns shown in Fig. 9, the speed standard deviation generally increases from the second to the fourth vehicle, indicating the gradual amplification of disturbances along the platoon. Although different vehicle models (e.g., the second vehicle is a Ford, while the following vehicles are Kia) exhibit different ranges of speed standard deviation, OPD generally results in lower or similar speed variability relative to TPD. The results also show how performance varies under different settings. In Segment 1 (high speed, small speed changes), OPD produces lower variability for the second and third vehicles and similar variability for the fourth vehicle. In Segment 2 (high speed, large speed changes), the differences between OPD and TPD are minimal. In Segment 3 (low speed, small speed changes), OPD consistently shows slightly lower variability across vehicles. In Segment 4 (low speed, large speed changes), OPD consistently shows much lower variability across vehicles, suggesting that OPD can provide smoother adjustments when substantial deceleration or acceleration occurs at lower speeds.

Fig. 10 shows the acceleration and deceleration distribution under ACC control over 3 following vehicles. Figs. 10a, 10c, and 10e show the acceleration distributions under four different speed profiles. Notably, the third and fourth vehicles exhibit more stable acceleration behavior under OPD mode. In contrast, the second vehicle behaves differently, which can be attributed to its distinct ACC control strategy. The Ford Mustang Mach-E (the second vehicle) adopts a more aggressive car-following response, resulting

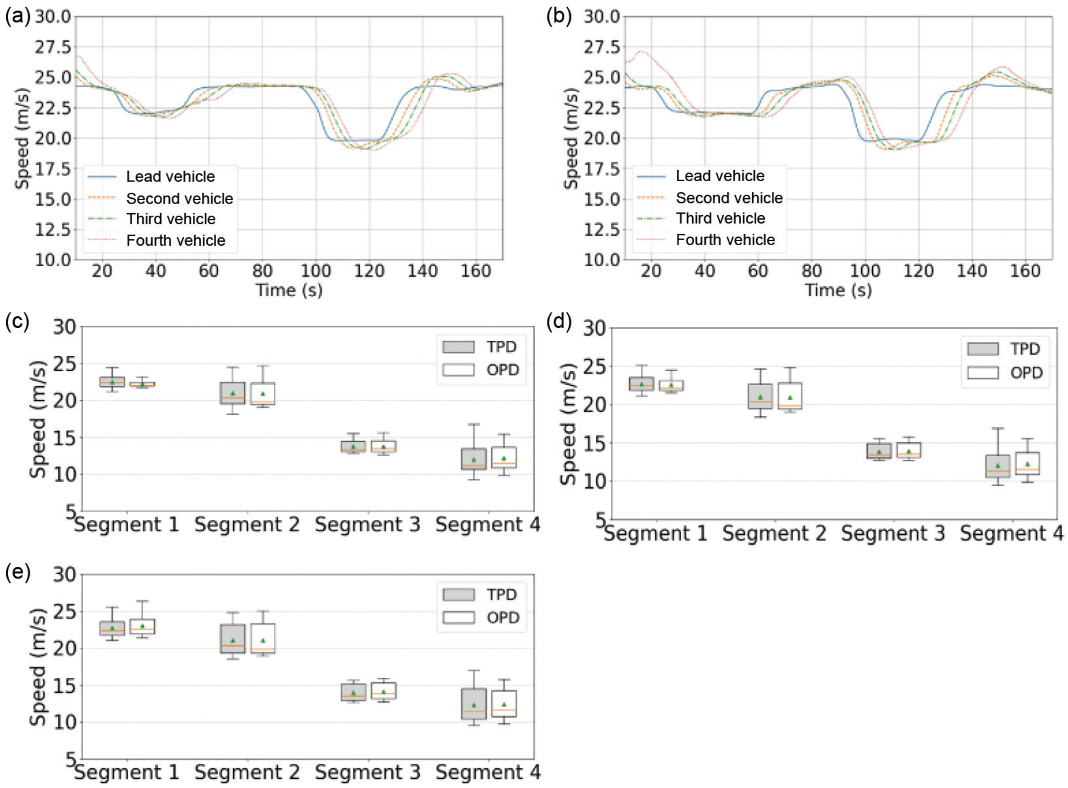

Fig. 9 Speed analysis in ACC: the speed trajectories in high-speed segments for (a) TPD and (b) OPD; (c–e) the corresponding speed distribution for the second, third, and fourth vehicles.

Table 8 Speed standard deviation of EVs in OPD and TPD modes

Segment	Mode	Second vehicle	Third vehicle	Fourth vehicle
Segment 1	OPD	0.698	0.878	1.542
Segment 1	TPD	0.977	1.194	1.470
Segment 2	OPD	1.827	2.000	2.234
Segment 2	TPD	1.840	1.993	2.185
Segment 3	OPD	0.818	0.945	1.056
Segment 3	TPD	0.895	1.037	1.171
Segment 4	OPD	1.789	1.942	2.160
Segment 4	TPD	1.917	2.057	2.199

in greater acceleration fluctuations, whereas the Kia Niro EVs demonstrate a more conservative behavior when the ACC is active. To explicitly separate pedal mode effects from vehicle-specific calibration, it is important to observe that while the acceleration range varies across models due to their distinct ACC tuning, the mean acceleration under OPD is consistently lower than that under TPD for all vehicles. This universal trend suggests that the reduction in acceleration intensity is a direct result of OPD logic rather than a byproduct of model heterogeneity. Figs. 10b, 10d, and 10f illustrate the deceleration distributions. Across all speed profiles, all vehicles exhibit more consistent and stable deceleration under OPD mode, indicating that the RBS exerts a stronger and more universal influence on longitudinal control when ACC is active.

Fig. 11 shows that the spacing distributions in OPD are generally more concentrated than those in TPD, reflecting reduced variability in spacing adjustments and indicating more stable and uniform car-following behavior across segments. Similar to the speed analysis, OPD results in lower spacing variability than TPD during smaller speed drops (Segments 1 and 3) and shows comparable variability during larger speed drops (Segments 2 and 4). Moreover, as speed oscillations amplify from the second to the fourth vehicle, spacing variability progressively increases and approaches that of TPD. These findings further support that the impact of OPD is influenced by the magnitude of speed oscillations. Integrating ACC with OPD is more effective at mitigating traffic oscillations than TPD, especially when the oscillation is small.

Furthermore, this study examine the influence of different headway settings. Fig. 12 shows the distribution of spacing under OPD and TPD across different headway settings. The spacing patterns appear similar between pedal modes. As expected, the longest headway setting consistently exhibits larger spacing compared to the shortest headway setting.

Overall, a clear contrast emerges when comparing OPD car-following behavior under ACC versus manual control. In the ACC scenarios, OPD results in noticeably narrower distributions of speed, acceleration, and spacing, especially in low-speed profiles, indicating smoother, more stable, and more conservative car-following behavior. This is attributed to the precise and consistent control provided by ACC, which eliminates variability from human inputs. In contrast, in the manual control scenarios, OPD exhibits amplified speed oscillations and greater variability in spacing and deceleration among downstream vehicles. These effects are likely due to driver heterogeneity and limited experience with OPD. The absence of tactile feedback and braking redundancy, where deceleration is controlled solely through the accelerator pedal, can lead to overcorrection, particularly in stop-and-go traffic.

The divergent performance of OPD under manual and ACC control is inherently linked to how the RBS interacts with the control source. In manual driving, the high sensitivity of the RBS acts as a source of instability because drivers tend to overcorrect during their initial encounter, amplifying human operational noise into larger oscillations. However, when the human element is replaced by ACC, this high sensitivity becomes an advantage. The ACC system can modulate the regenerative torque with high

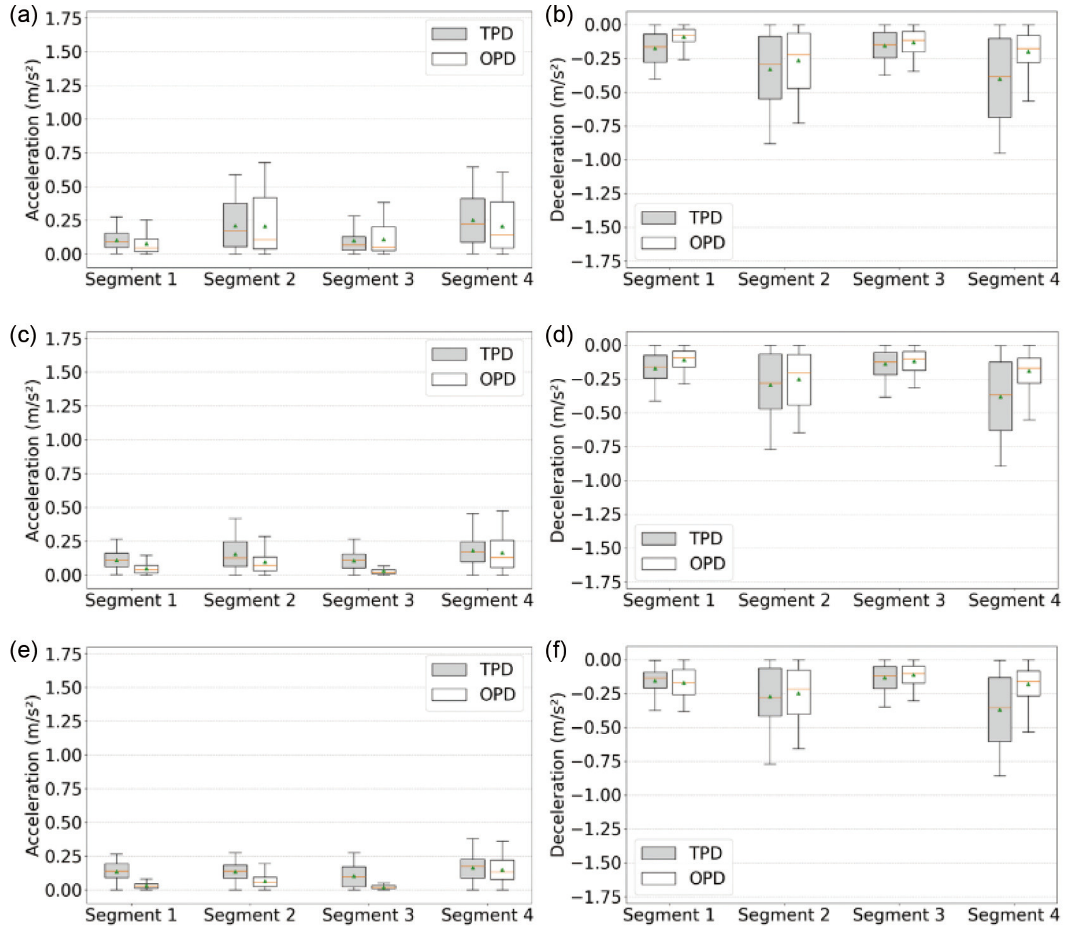

Fig. 10 Acceleration and deceleration distributions for TPD and OPD under ACC control and longest headway setting: the acceleration for (a) the second, (c) third, and (e) fourth vehicles; the corresponding deceleration distributions for (b) the second, (d) third, and (f) fourth vehicles.

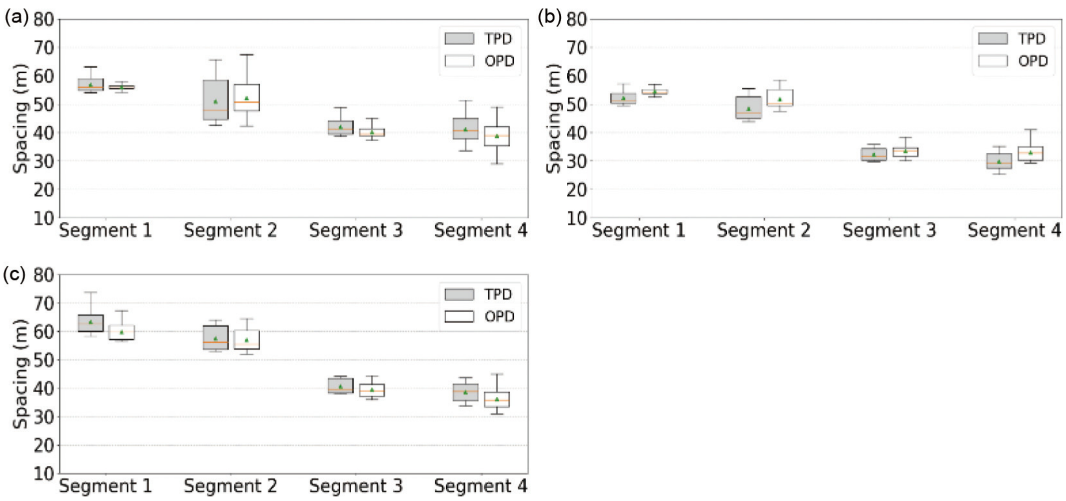

Fig. 11 Impact of headway settings on ACC with OPD and TPD: (a) the second, (b) third, and (c) fourth vehicles.

precision and zero mechanical transition time between accelerating and braking. This seamless control loop allows the OPD-equipped ACC to respond more conservatively to speed changes, thereby effectively mitigating traffic disturbances.

This observed trend—from oscillation-prone manual control with OPD to smooth, regulated behavior under ACC with OPD—highlights the importance of automation in maximizing the benefits of OPD. During the early stages of OPD adoption, drivers may require additional training to adapt to its unique control dynamics. Incorporating supportive safety features, such as visual feedback, adaptive deceleration cues, or transitional braking assistance, can further promote stable driving behavior and reduce variability. Moreover, while OPD offers advantages such as energy efficiency and simplified control, its full potential to improve comfort, flow stability, and safety is best realized when integrated with automated systems such as ACC.

5 Limitations and discussion

5.1 Study limitations

This study has several limitations that should be acknowledged.

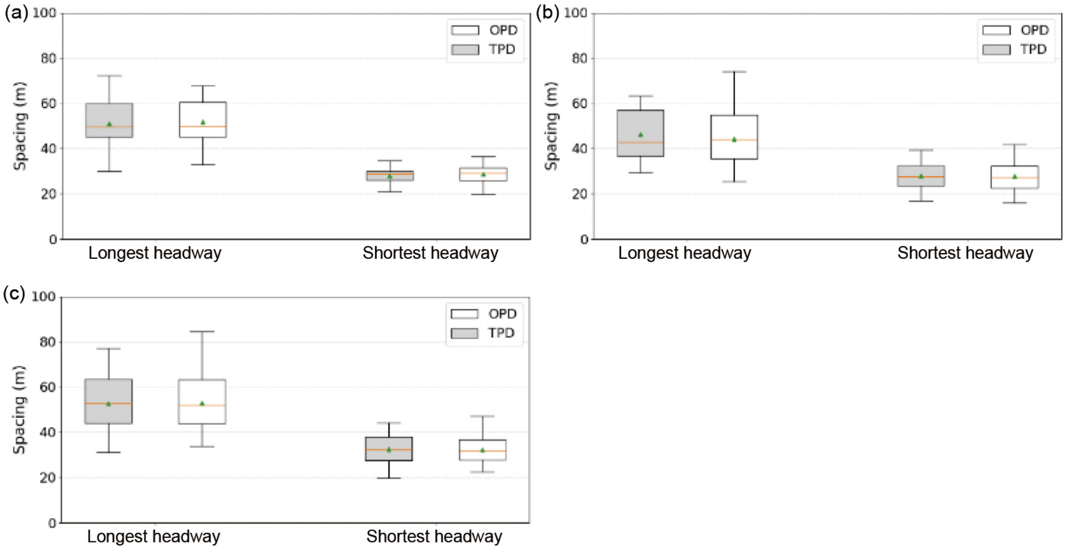

Fig. 12 Impact of headway settings on ACC with OPD and TPD: (a) the second, (b) third, and (c) fourth vehicles, respectively.

First, the sample size was relatively small, and all experiments were conducted with a limited number of drivers and vehicle types, which may restrict the generalizability of the findings. The participant pool may not fully represent the diversity of real-world EV drivers or vehicle models with different regenerative braking characteristics. Although the experiments were carefully controlled, potential biases related to the driver short-term adaptation effect to OPD and individual driving habits may have influenced the observed behavior. In addition, the results were obtained under specific road and traffic conditions, limiting external validity. More complex real-world environments with heterogeneous traffic and roadway conditions may lead to different behavioral responses.

Despite these limitations, several findings are expected to remain robust across broader populations. Specifically, the relative performance differences between manual control and ACC are likely to persist. ACC consistently mitigates traffic disturbances because its responses are governed by automated control logic that regulates spacing and speed adjustments in a systematic manner. In this sense, ACC can be viewed as an idealized control of manual car-following behavior, providing consistent and optimized responses that human drivers aim to approximate but rarely achieve consistently. Similarly, the intrinsic rapid deceleration response of OPD is determined by the system's physical and control design. Although different vehicle models were used in the field experiments, the findings on ACC and OPD remain consistent.

Conversely, the specific magnitudes of speed and spacing oscillations observed under manual OPD are highly sensitive to driver heterogeneity. Manual car-following behavior depends strongly on driver experience and pedal modulation skills, particularly when operating under OPD. As drivers become more familiar with OPD, they may learn to modulate acceleration and deceleration more smoothly. Consequently, the variance in manual driving performance is expected to decrease over time, and the resulting traffic flow characteristics may gradually approach those achieved by ACC.

5.2 Practical applications and discussion

Beyond experimental validation, the empirical data gathered in this study provide a crucial foundation for calibrating next-generation car-following models. Traditional models, such as the IDM, were primarily designed for ICE vehicles with distinct braking and acceleration inputs. Our findings suggest that OPD-specific behaviors can be incorporated into these models by adjusting the sensitivity parameters related to deceleration and spacing or by introducing a unified acceleration–deceleration function to reflect the single-pedal control structure. Specifically, the unique deceleration profiles and control variability observed in this study can be used to refine model parameters to better represent the high-sensitivity response of EVs. Integrating these OPD-specific behaviors into simulation platforms such as simulation of urban mobility (SUMO) or car learning to act (CARLA) will enable more realistic traffic flow modeling, allowing researchers to evaluate how increasing EV penetration affects string stability, safety, and throughput in traffic flow.

From an industrial perspective, these findings provide actionable insights for original equipment manufacturers (OEMs) to refine EV control interfaces. The performance gap between manual and ACC OPD suggests that manufacturers should prioritize enhanced pedal feedback mechanisms. By optimizing these design parameters based on the observed behavioral responses, OEMs can achieve smoother, more predictable vehicle deceleration, ultimately reducing driver fatigue and improving comfort in complex car-following scenarios.

At the system level, incorporating these behavioral insights into driver-assistance algorithms and infrastructure control strategies has strong potential to enhance overall transportation efficiency. For instance, vehicle-to-infrastructure (V2I) systems can utilize the specific deceleration characteristics of OPD vehicles to optimize signal coordination or speed harmonization strategies. By aligning infrastructure-based speed guidance with the natural regenerative braking curves of EVs, city planners can reduce traffic oscillations and improve energy recovery across the network. Ultimately, the synergy between OPD-aware algorithms and smart infrastructure can lead to a more stable, energy-efficient, and safer mobility ecosystem.

6 Conclusions

This study provides one of the first empirical investigations explicitly comparing EV car-following behaviors with OPD and TPD under both manual control and ACC settings.

In manual car-following, distinct behavioral differences emerge between OPD and TPD. OPD produces larger fluctuations in speed and acceleration—especially at low speeds—while TPD yields smoother and more consistent control. Deceleration under OPD is quicker, reflecting the difficulty of balancing both braking and acceleration using a single accelerator pedal. Spacing results further show greater variability under OPD, particularly in low-speed segments. Importantly, this variability is driven by both the inherent sensitivity of the single pedal system and a short-term adaptation effect for drivers accustomed to traditional TPD.

Under ACC, significant behavioral differences were also observed between OPD and TPD. Both modes exhibit similar response delays, demonstrating the ability of ACC to effectively manage longitudinal control without human inputs. Notably, although different EV models were used, the shift toward smoother and more conservative behavior under OPD is consistent across all vehicles, suggesting that these effects are independent of vehicle-specific ACC implementations. OPD tends to produce narrower speed, acceleration, and spacing distributions, indicating smoother and more conservative vehicle responses. Furthermore, OPD outperforms TPD in handling small speed fluctuations and exhibits similar behavior when fluctuations are large. This suggests that integrating OPD with ACC can help mitigate traffic disturbances, leading to improved stability and smoother traffic flow.

Overall, this study reveals a clear contrast between OPD car-following behavior under manual control and ACC, underscoring the critical role of automation in overcoming transitional control challenges and unlocking the full benefits of OPD. To support early adoption and ease this learning phase, driver training and the inclusion of supportive safety features, such as visual feedback and adaptive deceleration cues, are recommended. Integrating OPD with ACC can improve driver comfort, reduce traffic oscillations, and enhance safety in transportation systems.

In future work, additional experiments will be conducted to further investigate OPD car-following behavior. These will incorporate multiple OPD settings—such as low, intermediate, and high regenerative braking levels. More diverse scenarios would be conducted, including congested urban areas and signalized corridors, with more complex traffic conditions. In addition, a wider range of vehicle brands and models are involved to examine how variations in regenerative braking design and calibration across manufacturers influence stability, comfort, and control variability. Repeated trials will be performed for each configuration to enhance experimental reliability, particularly under manual control. Importantly, we plan to leverage these empirical findings to develop and calibrate OPD-specific car-following models, such as the IDM, and derive analytical relationships to explain control behavior differences across various speed scenarios. Repeated trials will be performed for each configuration to enhance experimental reliability, particularly under manual control. Moreover, future studies with a broader participant pool, including drivers with different levels of OPD familiarity, will help clarify the human-control factors underlying these behavioral differences.

Author contributions

Tianle Zhu: Data collection and processing, Analysis and interpretation of results, Draft manuscript preparation. **Handong Yao**: Study conception and design, Data collection and processing, Analysis and interpretation of results, Manuscript review. **Wenjie Zhao**: Data collection and processing, Manuscript review. **Qianwen Li**: Data collection and processing, Manuscript review.

Replication and data sharing

The data used in this study are available at https://doi.org/10.26599/ETSD.2026.9190013.

Declaration of competing interest

The authors have no competing interests to declare that are relevant to the content of this article.

References

Brackstone, M., McDonald, M., 1999. Car-following: A historical review. *Transp Res Part F Traffic Psychol Behav*, **2**, 181−196.

Chon Kan-Munoz, P., Lapardhaja, S., Kan, X. D., 2021. Field experiments of commercially available automated vehicles on freeways. Transportation Research Board. TRBAM-21-03778.

Fayolle, G., Lasgouttes, J. M., Flores, C., 2022. Stability and string stability of car-following models with reaction-time delay. *SIAM J Appl Math*, **82**, 1661−1679.

Gunter, G., Gloudemans, D., Stern, R. E., McQuade, S., Bhadani, R., Bunting, M. et al., 2020a. Are commercially implemented adaptive cruise control systems string stable? *IEEE Trans Intell Transport Syst*, **22**, 6992−7003.

Gunter, G., Janssen, C., Barbour, W., Stern, R., Work, D., 2020b. Model-based string stability of adaptive cruise control systems using field data. *IEEE Trans Intell Veh*, **5**, 90−99.

Hamada, A. T., Orhan, M. F., 2022. An overview of regenerative braking systems. *J Energy Storage*, **52**, 105033.

Lapardhaja, S., Yagantekin, K. U., Yang, M., Majumder, T. A., Kan, X., Badhrudeen, M., 2023. Unlocking potential capacity benefits of electric vehicles (EVs) with adaptive cruise control (ACC). *Transp B Transp Dyn*, **11**, 1894−1911.

Li, X., 2022. Trade-off between safety, mobility and stability in automated vehicle following control: An analytical method. *Transp Res Part B Methodol*, **166**, 1−18.

Li, Y., Liang, Z., Zhu, H., Tang, X., 2019. Electric vehicle dynamics-based car-following model and stability analysis. In: 2019 Chinese Control Conference (CCC), 6692−6696.

Li, Z., Bian, Z., Chen, Z., Ozbay, K., Zhong, M., 2024. Synthesis of electric vehicle charging data: A real-world data-driven approach. *Commun Transp Res*, **4**, 100128.

Liu, Y., Wu, F., Liu, Z., Wang, K., Wang, F., Qu, X., 2023. Can language models be used for real-world urban-delivery route optimization? *Innovation*, **4**, 100520.

Ma, J., Zhang, X., Xu, W., Li, J., Gong, Z., Zhao, J., 2025. One-pedal or two-pedal: Does the regenerative braking system improve driving safety? *Accid Anal Prev*, **210**, 107832.

Milanés, V., Shladover, S. E., 2014. Modeling cooperative and autonomous adaptive cruise control dynamic responses using experimental data. *Transp Res Part C Emerg Technolog*, **48**, 285−300.

Newell, G. F., 2002. A simplified car-following theory: A lower order model. *Transp Res Part B Methodol*, **36**, 195−205.

Orosz, G., Wilson, R. E., Stépán, G., 2010. Traffic Jams: Dynamics and control. *Phil Trans R Soc A*, **368**, 4455−4479.

Rajamani, R., 2006. Vehicle Dynamics and Control. New York: Springer.

Ruan, T., Lv, Q., 2022. Public perception of electric vehicles on reddit over the past decade. *Commun Transp Res*, **2**, 100070.

Taylor, J., Zhou, X., Rouphail, N. M., Porter, R. J., 2015. Method for investigating intradriver heterogeneity using vehicle trajectory data: A dynamic time warping approach. *Transp Res Part B Methodol*, **73**, 59−80.

Treiber, M., Hennecke, A., Helbing, D., 2000. Congested traffic states in empirical observations and microscopic simulations. *Phys Rev E*, **62**, 1805−1824.

Wang, J. J., Besselink, I., van Boekel M. A. J. S., Nijmeijer, H., 2015. Evaluating the energy efficiency of a one pedal driving algorithm. In: 2015 European Battery, Hybrid and Fuel Cell Electric Vehicle Congress (EEVC 2015),1−10.

Wang, Y., Witlox, F., 2025. Global trends in electric vehicle adoption and the impact of environmental awareness, user attributes, and barriers. *Energy Rep*, **13**, 1125−1137.

Zare, A., Shang, M., Kan, X., Stern, R., 2023. Modeling car-following behavior of electric adaptive cruise control vehicles using experimental testbed data. *IEEE Intell Transp Syst Conf*, **2023**, 5585−5590.

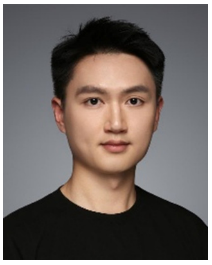

Tianle Zhu received the M.E. degree in computer science from the University of Florida, Gainesville, USA, and the B.S. degree in computer science and technology from Nanjing Forestry University, Nanjing, China. He is currently pursuing the Ph.D. degree in mechanical engineering at the University of Georgia, USA. His research interests include traffic modeling, machine learning, and cooperative perception.

Handong Yao received the Ph.D. degree in transportation engineering from the Harbin Institute of Technology, China. He is an Assistant Professor in the College of Engineering at the University of Georgia. His research is mainly focused on developing cyber-physical transportation systems with smart infrastructure technologies and AI techniques and using machine learning methods and traffic flow theory to improve system sustainability, safety, and efficiency.

Wenjie Zhao received the M.E. degree in systems science and the B.S. degree from Beijing Jiaotong University, Beijing, China. She is currently pursuing the Ph.D. degree in civil engineering at the University of Georgia, USA. Her research focuses on intelligent transportation systems, with a particular emphasis on transportation modeling and autonomous vehicle applications.

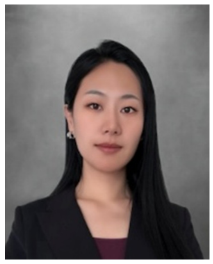

Qianwen (Cami) Li received the Ph.D. degree in civil engineering (transportation) from the University of South Florida. She is the Assistant Professor in the School of Environmental, Civil, Agricultural, and Mechanical Engineering (ECAM) at the University of Georgia. Her research focuses on enhancing transportation safety and efficiency using emerging technologies such as vehicle automation, communication, electrification, and smart infrastructure.